Biochemical Genetics
https://doi.org/10.1007/s10528-022-10325-1

ORIGINAL ARTICLE

Wild-type IDH1 Knockout Leads to G0/G1 Arrest, Impairs Cancer Cell Proliferation, Altering Glycolysis, and the TCA Cycle in Colon Cancer

Esra Bulut Atalay[1,2] · Serif Senturk[1,2] · Hulya Ayar Kayali[1,2,3]

Received: 26 June 2022 / Accepted: 28 December 2022

Abstract

The isocitrate dehydrogenase (IDH), which participates in the TCA cycle, is an important key enzyme in regulating cell metabolism. The effect of the metabolic IDH enzyme on cancer pathogenesis has recently been shown in different types of cancer. However, the role of wild-type (wt) IDH1 in the development of colon cancer is still unknown. Our study investigated the role of the IDH1 enzyme in key hallmarks of colon cancer using various methods such as wound healing, cell cycle, colony formation ability, invasion, and apoptosis analysis. Furthermore, cell metabolism was investigated by pyruvate analysis, dinitrosalicylic acid, and HPLC methods. In addition, CRISPR/Cas9 tool was utilized to knockout the IDH1 gene in colon adenocarcinoma cells (SW620). Further studies were performed in two isogenic IDH1 KO clones. Our findings in both clones suggest that IDH1 KO results in G0/G1 arrest, and reduces proliferation by approximately twofold compared to IDH1 WT cells. In addition, the invasion, migration, and colony formation abilities of IDH1 KO clones were significantly decreased accompanied by significant morphological changes. In the context of metabolism, intracellular glucose, pyruvate, αKG, and malate levels were decreased, while the intracellular citrate level was increased in IDH1 KO clones as compared to IDH1 WT cells. Our results reveal that wt IDH1 knockout leads to a decrease in the aggressive features of colon cancer cells. In conclusion, we reported that wt IDH1 has an effective role in colon cancer progression and could be a potential therapeutic target.

Keywords Colon cancer · Glycolysis · Knockout · TCA cycle · Wild-type IDH1 · IDH1 silencing · CRISPR/Cas9 method · Metabolism · Therapeutic target

Abbreviations

IDH Isocitrate dehydrogenase

✉ Hulya Ayar Kayali
hulya.kayali@deu.edu.tr

Extended author information available on the last page of the article

Published online: 12 January 2023

wt	Wild-type
FH	Fumarate hydratase
SDH	Succinate dehydrogenase
αKG	α-Ketoglutarate
MeOH	Methanol
DNS	Dinitrosalicylic acid
DNPH	2,4-Dinitrophenylhydrazine
TBS	Tris-buffered saline
RT-qPCR	Reverse transcriptase quantitative polymerase chain reaction

Introduction

Cancer is a disease in which cells undergo metabolic and behavioral changes as a result of mutations in a multistage process. These changes occur due to modifications of the mechanisms that control cell proliferation and survival. The cancer cells adapted to have the ability to obtain the necessary nutrients from the environment and use these nutrients to build new biomass and maintain cellular bioenergetics (Hanahan 2022). During carcinogenesis, many cancer cells exhibit similar functional properties through diverse mechanisms. Limitless division, metabolic rearrangement, escaping apoptosis, invasion, and metastasis acquisition are some of the hallmarks of cancer (Hanahan and Weinberg 2011). As is known, there are more than 200 types of cancer and colon cancer is the 3rd most common cancer type in both men and women and 2nd type of cancer that causes death (Xi and Xu 2021). According to GLOBOCAN data, 1.15 million new colon cancer cases were observed in 2020, and unfortunately, approximately 940 thousand patients died. With these values, colon cancer accounted for 10% of the total cancer incidence and 9.4% of all cancer-related deaths (Sung et al. 2021). Until now, colon cancer metastasis, and genomic remodeling were investigated to find a new therapeutic target molecule (Wen et al. 2020; Shi et al. 2022; Hao et al.2022). Patients' survival rates have not improved despite advanced metastatic surgery and improved treatment alternatives, highlighting the need for novel therapeutic methods. The development of an effective systemic therapy related to the metabolic rearrangement of colon cancer may give a new perspective to cancer treatments (Neitzel et al. 2020; Bin et al. 2022).

Cancer cells exhibit atypical metabolic features in energy production reactions such as glycolysis and the TCA cycle. In addition to energy production, precursors synthesized with TCA intermediates are the basic building blocks of the cell (Krebs and Johnson 1937). Earlier studies indicate that some metabolic enzymes such as fumarate hydratase (FH) (Crooks et al. 2021), succinate dehydrogenase (SDH) (Hao et al. 2009), and IDH (Dang et al. 2009) involved in the TCA cycle have been found to have an active role in cancer development. IDH enzymes perform decarboxylation of isocitrate to α-ketoglutarate (αKG), which further oxidizes to the succinate and produces NADH (Barnes et al. 1971). IDH, a key enzyme in the TCA cycle, has three isoforms (Dalziel 1980). The $NADP^+$-dependent IDH1 and IDH2 isoforms are homodimeric and catalyze the reversible reaction. IDH1 is found in the cytoplasm, whereas IDH2 carries out the same reaction in the mitochondria. IDH1 isoforms

have essential roles such as the generation of NADPH and participating in glucose and lipid metabolism (Pollard and Ratcliffe 2009). As is known in the previous studies, IDH1 overexpress in various cancer types including colon cancer (Yang et al. 2021). Since the discovery of IDH mutations that lead to 2-hydroxyglutarate (2-HG) oncometabolite production (Dang et al. 2009), studies in this field have provided a better characterization of the role of IDH1 enzymes in tumorigenesis (Su et al. 2020; Li et al. 2019; Biedermann et al. 2019). Because the incidence of mutation in colon cancer is very low (Sjöblom et al. 2006), studies have been focused on wt-IDH enzymes (Wang et al. 2020; Qiao et al. 2021). However, the role of the wt-IDH1 enzyme in the context of colon carcinogenesis has not been studied until now.

CRISPR/Cas9 method is based on Cas9-sgRNA mediated cleavage of a target DNA sequence resulting in the knockout of the target gene (Jinek et al. 2012). Although there is more than one method for genome editing, the CRISPR/Cas9 method has become the most popular due to its advantages, such as simplicity, adaptability, and low off-target effect (Wu et al. 2020; Alavi and Rai 2021). In the present study, the IDH1 enzyme was knocked out in colon adenocarcinoma cells (SW620) using the CRISPR/Cas9 method. The wt-IDH1 gene was successfully depleted in two clones (IDH1 KO1 and KO2). Our molecular studies found that IDH1 knockout affected the significant hallmarks of colon cancer such as proliferation, invasion, migration, and metabolic rearrangement. Notably, specific alterations were observed in the cell morphology of IDH1 KO clones. Our study showed that wt-IDH1 could be a potential therapeutic target in colon cancer.

Material and Methods

Cell Culture

Kidney (HEK293T) and metastatic colon adenocarcinoma cells (SW620) cultured in RPMI-1640 medium were used. As previously described, cell culture conditions were applied (Subasi et al. 2020).

Extraction of Intracellular and Extracellular Metabolites

One million of each cell line was seeded into 4 Petri dishes. After 24–96 h, 1 ml of medium was taken from each petri dish and centrifuged at 17,000 g and + 4 °C for 15 min. The supernatants were kept at − 80 °C until analysis. The consumed and released metabolite levels in the growth medium were calculated in 1 million cells as described in our previous article (Atalay and Kayalı 2022).

After seeding 1 million cells, the cell number was calculated in 24–96 h. 100 µl of cold 50% methanol (MeOH): water (1:1) solution for 1 million cells were added to the cell pellet. Cells were lysed in an ultrasonic bath for 30 s and then incubated on ice for 10 min. The lysates were centrifuged at 17,000 g and + 4 °C for 15 min.

The supernatant was used for analysis (Atalay and Kayalı 2022). Experiments were carried out three independent times.

DNS (Dinitrosalicylic Acid) Method

DNS method was used to determine the reducing glucose content in the cell pellets and growth media (Khuwijitjaru et al. 2017) as described in our previous article (Atalay and Kayalı 2022).

Pyruvate Content Analyses

The existing protocol in the literature has been optimized to 100 µL (96 well plates) (Yoo et al. 2011). 10 µl of 2,4-dinitrophenylhydrazine (DNPH) solution and 30 µl of samples were added to each well and incubated for 5 min at room temperature. Next, 60 µl of 2 N sodium hydroxide (NaOH) was added and incubated again at room temperature for 10 min. Samples and standard pyruvate solutions were measured using a spectrophotometer at 520 nm absorbance.

Analyzing Metabolites with HPLC

The HPLC (Agilent) system used to have an Alltech OA-1000 column, a UV detector, and a differential refractive index detector. The mobile phase (0.4 mL/min) was 9.0 mM H_2SO_4 solution and the column was run at 42 °C. The UV detector (210 nm) was used to detect citrate, αKG, fumarate, and malate standards (Ayar Kayali and Tarhan 2006).

Western Blotting

Cell pellets were subjected to physical lysis by sonication for 30 s in RIPA buffer and incubated on ice for 15 min. The supernatant was obtained after centrifugation at 13,300 rpm for 15 min at 4 °C. The cell lysates were mixed in a 3:1 ratio with an SDS-PAGE loading buffer and incubated at 95 °C for 15 min. The samples were loaded with 30 µg of protein and run at 100 V for 2 h on 12% SDS-PAGE gels. The samples were then transferred to a nitrocellulose membrane at 250 mA for 1.5 h. Membranes cut according to the appropriate protein weight were blocked in 1% BSA or milk powder according to the used antibodies for 45 min and then washed three times with Tris-buffered saline (TBS) solution containing 0.1% Tween-20. Then, it was incubated for 2 h with the IDH1 and GAPDH primary antibody solutions prepared in a blocking buffer under room conditions. Next, the membranes were rinsed three times with TBST solution before being incubated for 1 h with a blocking buffer-prepared HRP-conjugated secondary antibody solution. The membranes were then washed three times with TBST solution before being visualized using the ECL western blotting analysis technique (Subasi et al. 2020).

Table 1 sgRNAs selected for IDH1 gene

	Forward (5′–3′)	Reverse (5′–-3′)
sgRNA1	CACCGCATAGGTCGTCAT GCTTATGG	AAACCATAAGCATGACGACCTATGC
sgRNA2	CACCGTCATAGGTCGTCA TGCTTATG	AAACATAAGCATGACGACCTATGAC

CRISPR/Cas9 Method

The sequences of two different sgRNAs selected from the Brunello library are listed in Table 1. Ligation of the phosphorylated oligos and 50 ng of Lenti CRISPR V2 vector was performed in 2 h at room temperature. The plasmid containing the Renilla gene was used as a control. The ligation product was transformed into competent E.coli bacteria (Stbl3) by the heat-shock method, and three clones were selected. Plasmid isolation was performed with NucleoSpin Plasmid QuickPure™ Kit, and their sequences were validated by the Sanger method.

Virus production and transfection: The plasmid mix containing gRNA (lenti CRISPR V2), psPAX2, and pMD2G plasmids (4:2:1) was prepared in the growth medium. PEI transfection agent was added as 5 µl to 1 µg DNA. After 30 min of incubation at room temperature, HEK293T cells in the 6-well plates were transfected dropwise with the plasmid mix. After 48 h, the medium was filtered with the 0.22 µm filter, and SW620 cells were infected at a ratio of 1:10. Polybrene was applied with a final concentration of 8 µg to increase the infection efficiency. 2 days after infection, cells were stained with DAPI dye, and GFP^+ cells were sorted by FACS analysis. Single cells were first seeded in a 96-well plate. Then,

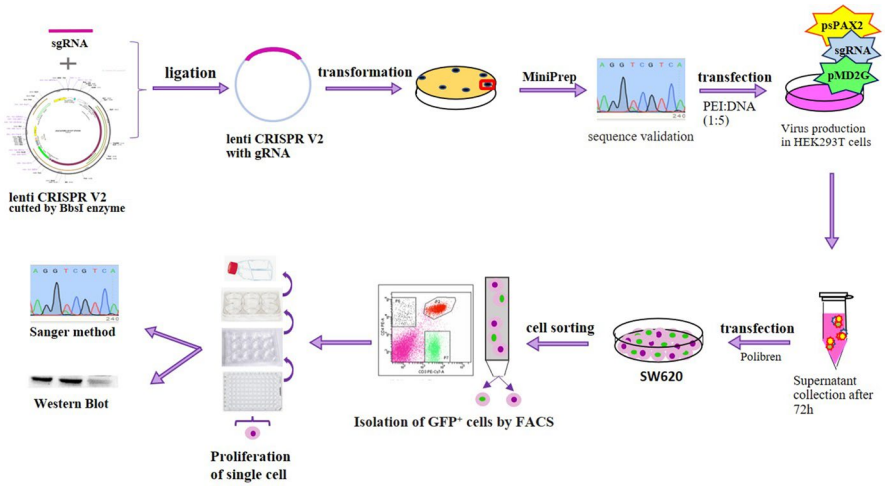

Fig. 1 The schematic presentation of the knockout of the IDH1 gene using the CRISPR/Cas9 method

colony formation from a single cell was imagined with Cell Metric™. Clones proliferated from a single cell were plated in 24 wells, 6 wells, and then in a petri dish, respectively (Ran et al. 2013) (Fig. 1).

Colony formation assay

10×10^4 cells were seeded in a 6-well plate/per well and incubated for 14 days in RPMI with 10% FBS. Clones were fixed with 4% formaldehyde for 20 min. The PBS-washed clones were stained with 0.1% crystal violet for 30 min. After washing with distilled water, clones were imagined using a stereomicroscope, and clone numbers were counted by Image J software (Franken et al. 2006).

Cell Proliferation

For cell proliferation studies, 1×10^6 cells were seeded per 100 mm diameter dish. After 24–96 h, cells in a petri dish were counted using a hemocytometer under a light microscope.

Migration Assay

3×10^5 cells were seeded in the 12 well plates. After 24 h, a linear wound was created by scratching the surface of the per well using a yellow pipette tip and incubating in RPMI with %1 FBS. The wounds were imaged, and their distance was measured using an inverted microscope.

DNA İsolation and Polymerase Chain Reaction (PCR)

DNA isolation was performed with the DNeasy Blood & Tissue Kit (Qiagen) as specified in the kit procedure. The purity of the DNA obtained using the kit was determined by the nanodrop device (Thermo). Target DNA sequences were amplified by PCR reaction for sequencing. Reverse and forward primers designed for the IDH1 enzyme are given in Table 2. PCR reaction was performed under the conditions specified in the OneTaq® Quick-Load® 2X Master Mix kit protocol (Table 3). PCR products were sequenced with the Sanger Method.

Table 2 Primer sequences. The primers were designed for the IDH1 enzyme for PCR analysis

Enzyme	Forward (5′–3′)	Reverse (5′–3′)
IDH1	GATGCCACCAACGACCAAGTC	GTGTTGAGATGGACGCCTATTTGTAAG

Table 3 The PCR conditions

Step	PCR				
	Initial Denaturation	30 cycles			Final Extension
		Denature	Anneal	Extension	
Time	30 s	15 s	30 s	30 s	5 min
Temp (°C)	94	94	62	68	68

Table 4 The RT-qPCR conditions

Step	Enzyme Activation	PCR	
	Hold	40 cycles	
		Denature	Anneal/Extend
Time (sec)	120	15	30
Temp (°C)	95	95	60

Table 5 The sequences of primers designed for RT-qPCR analysis

Enzyme	Forward (5′–3′)	Reverse (5′–3′)
IDH1	CGGTCTTCAGAGAAGCCATT	AGGCCCAGGAACAACAAAAT
GAPDH	GGTGTGAACCATGAGAAGTATGA	GAGTCCTTCCACGATACCAAAG

Reverse Transcriptase Polymerase Chain Reaction (RT-PCR)

Total RNA was extracted from 3×10^6 cells with TRI Reagent (Ambion), and their quantification was detected with Nanodrop (Thermo). Then, 1 µg RNA was converted to cDNA with the High-Capacity RNA-to-cDNA Kit. For quantitative RT-PCR (Table 4), the GoTaq master mix (A6002) was used. The internal standard was GAPDH, and the relative quantification was calculated using the $2^{-\Delta\Delta Ct}$ method (Livak and Schmittgen 2001). Table 5 contains the primer sequences for the IDH1 and GAPDH genes.

Cell İnvasion

The invasion abilities of cells were evaluated using a QCM™ 24-Well Cell Invasion Assay (Chemicon). Experiments were performed as described in the kit protocols.

Cell Cycle

Cell cycle analysis was performed as previously described, and the results were analyzed by the FlowJo program (Subasi et al. 2020).

Apoptosis Analysis

The Alexa FluorR488 Annexin V/Dead Cell Apoptosis (Invitrogen) kit was used to identify cells that tended to apoptosis after the depletion of the IDH1 gene. Experiments were performed as described in the kit protocols.

Statistical analysis

The experiments were repeated at least three times, and the results are mean ± SD of at least three independent experiments. Statistical analyzes were carried out using GraphPad Prism 8.0 (GraphPad Software, CA, USA). Statistically significant $p < 0.05$ values determined using the One-way analysis of variance (ANOVA) followed by Tukey's multiple comparisons test were indicated by an asterisk (*) symbol on the graph.

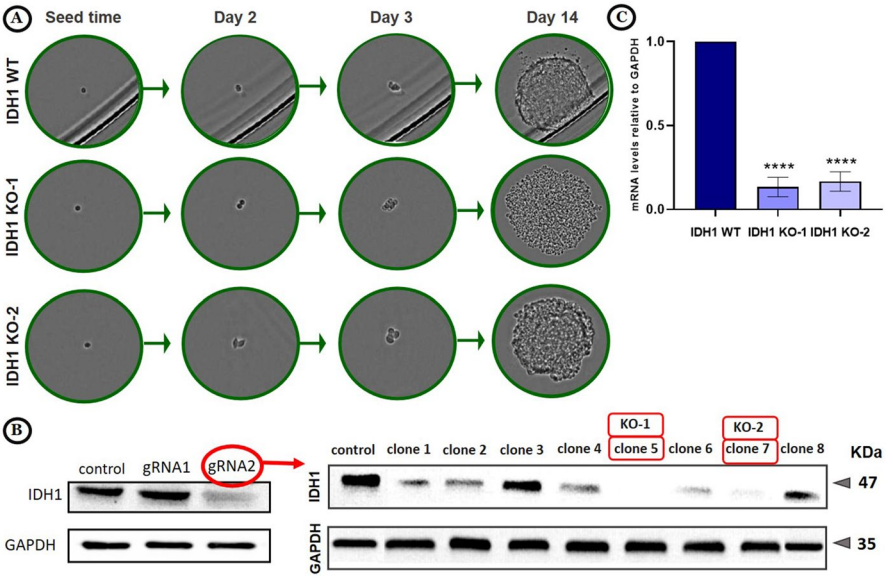

Fig. 2 The validation of IDH1 knockout using the CRISPR/Cas9 method. **A** After transfection, colony formation from a single cell was imagined for 14 days with Solentim Cell Metric™. **B** The protein levels of IDH1 in the bulk population and the 8 different colonies were determined using Western blot analysis. **C** RT-qPCR was used to determine the mRNA level of IDH1 genes. GAPDH was control. ***$p < 0.001$, ****$p < 0.0001$

Results

Knocking out of the wt IDH1 gene by CRISPR/Cas9 method

The CRISPR/Cas9 method was carried out with the lentiviral (CRISPRv2) vector. Two different gRNAs were selected from the Brunello library targeting the 4th exon of the IDH1 gene. Colony formation from a single cell was imagined using Solentim Cell Metric™ for 14 days after transduction of gRNA-containing lentiCRISPRv2 vectors into cells (Fig. 2A). Firstly, the bulk population of both gRNAs was analyzed. Then, the decreased IDH1 protein level was determined in the cells which carry gRNA2, and single-cell clones were propagated. Protein levels of IDH1 were completely reduced in 2 clones, and these clones were named IDH1 KO-1 and IDH1 KO-2 (Fig. 2B). The IDH1 gene sequences of the clones were validated by the Sanger method. The results were evaluated with Mutation Surveyor Software, and the deletions of "TCGTCA" in IDH1 KO-1 and "A" in IDH1 KO-2 were determined (data not shown). In addition, mRNA levels of the IDH1 were examined by the RT-qPCR method, and it was significantly decreased in IDH1 KO clones compared to the control (Fig. 2C).

The effect of IDH1 Knockout on Morphology, Proliferation, Colony Formation, İnvasion, and Migration of SW620 Cells

The changes in the cell morphology were examined with an inverted microscope. The wt IDH1 cells have both rounded and fibroblast-like (red arrow) morphology. However, IDH1 knockout cells displayed only rounded morphology (Fig. 3A).

The affect of IDH1 gene knockout on cell proliferation was investigated. It was observed that the cell number in IDH1 KO-1 and IDH1 KO-2 were 1.5- and 1.6-fold decreased at the end of the fourth day compared to the control group, respectively (Fig. 3B). As is shown, IDH1 gene depletion inhibited cell proliferation.

The invasion abilities of IDH1 KO clones were evaluated using a transwell assay. Cells invaded from the top chamber in the lower chambers were stained and detected with a fluorometric measurement. The relative invasion rates of IDH1 KO-1 and IDH1 KO-2 cells were decreased by 2.4- and 2.0-fold, respectively (Fig. 3C).

To evaluate the migration abilities of cells after IDH1 knockout, a linear wound was generated by the yellow (200 µl) pipet tip. The images were taken, and the distances were measured with inverted microscopy for 4 days. The distance in IDH1 KO-1 and IDH1 KO-2 was 19.8% and 18.6%, respectively, while it was 11.2% in IDH1 WT at the end of the 4th day, suggesting that the migration abilities of IDH1 KO cells were decreased when compared to wt IDH1 cells (Fig. 4A-B).

Next, to determine how IDH1 knockout affects the colony formation ability of SW620 cells, the colonies were counted after 15 days. The number of colonies formed by IDH1 KO1-2 cells decreased to 55.8% and 60.8%, respectively (Fig. 4C). As is shown, knocking out the wt IDH1 led to reduced colony formation.

The effect of IDH1gene knockout in the distribution of cell cycle phases was analyzed after cells were stained with PI dyes, and the number of cell cycle phases

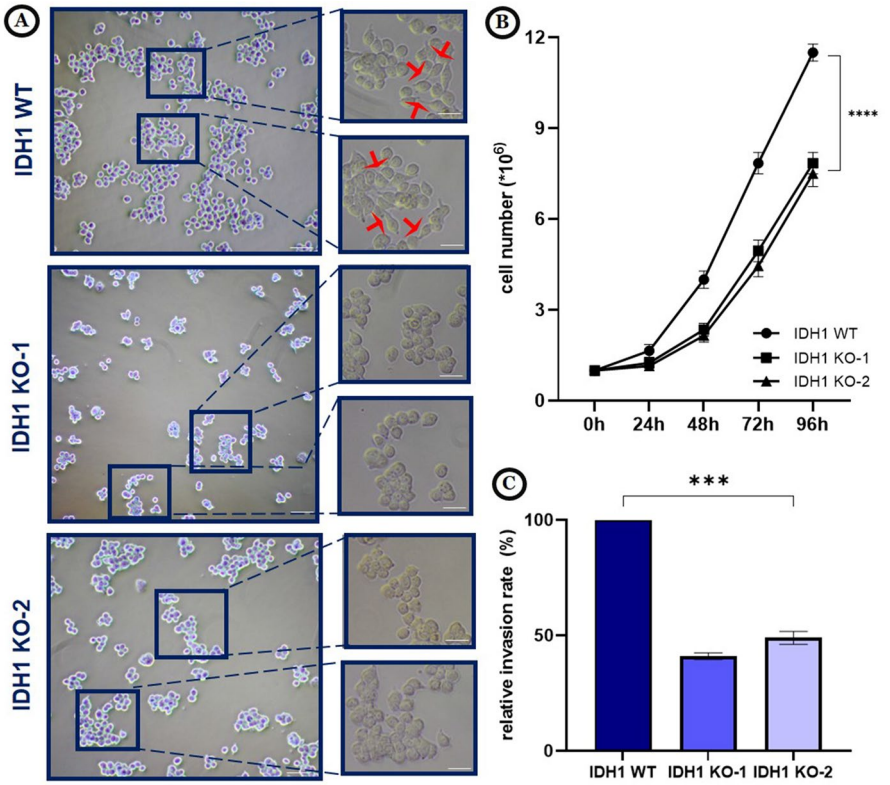

Fig. 3 IDH1 promote the proliferation of colon adenocarcinoma cells. **A** The morphological imaging of IDH1 WT and IDH1 KO cells was analyzed with inverted microscopy with 10X and 20X. The scale bar is 200 µm. **B** The effect of IDH1 knockout on cell proliferation during 4 days. **C** The invasion abilities of IDH1 WT and IDH1 KO 1–2 cells were evaluated using a transwell assay. At the end of 24 h, the cells invaded from the top chamber in the lower chambers were detected, and invasion rates were determined relative to the control group. ***$p < 0.001$, ****$p < 0.0001$, ns: non-significant

was determined by the FlowJo program. As seen in Fig. 5A, while the cell density kept in the G phase was 55% in the IDH1 WT, it was increased to 72% and 73% in IDH1 KO-1 and IDH1 KO-2 clones, respectively. Concerning this, while the cell density in the S phase was 20% in the control group, it decreased to 9% and 11% in IDH1 KO-1 and IDH1 KO-2 clones, respectively. Similarly, while the cell density in the G2/M phase was 25% in the control group, it decreased to 18% and 17% in IDH1 KO-1 and IDH1 KO-2 colonies, respectively (Fig. 5A). It is shown that IDH1 knockout led to G0/G1-phase arrest.

Lastly, to determine the apoptosis effect of IDH1 silencing, cells were stained with Annexin V and PI dyes, and the results were analyzed with the FlowJo program. The Q1and Q2 parts show the number of cells in necrosis or late apoptosis and early apoptosis, respectively. The number of cells undergoing apoptosis did not change in both IDH1 KO clones when compared to the control group (Fig. 5B).

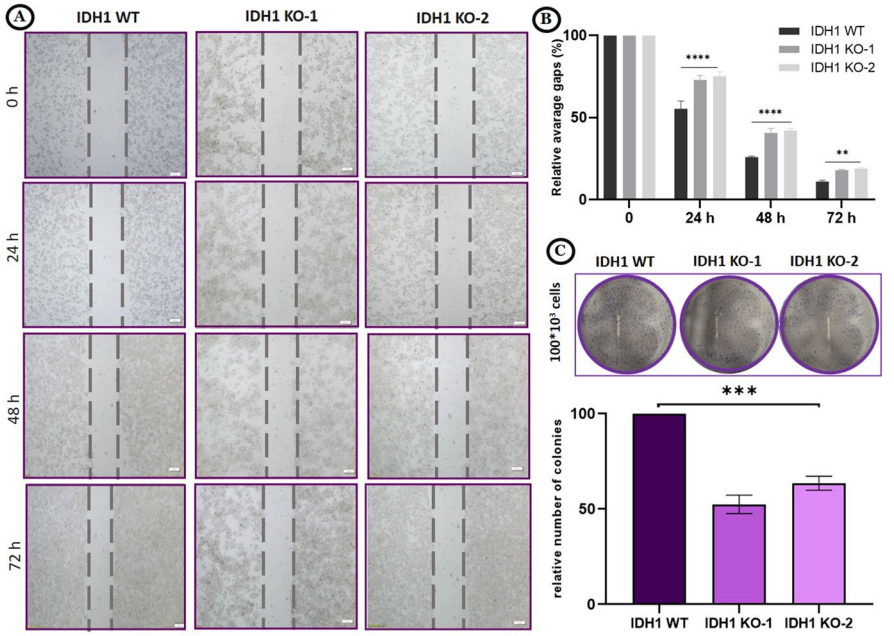

Fig. 4 IDH1 knockout led to a decrease in colony formation ability and migration of SW620. **A** Wound healing assay was used to determine cell migration ability in IDH1 WT and IDH1 KO1-2 cells. **B** The average gaps were determined relative to the control group. **C** Colony formation ability after IDH1 knockout was evaluated by counting colonies stained with crystal violet. $^{**}p < 0.01$, $^{****}p < 0.0001$, ns: non-significant

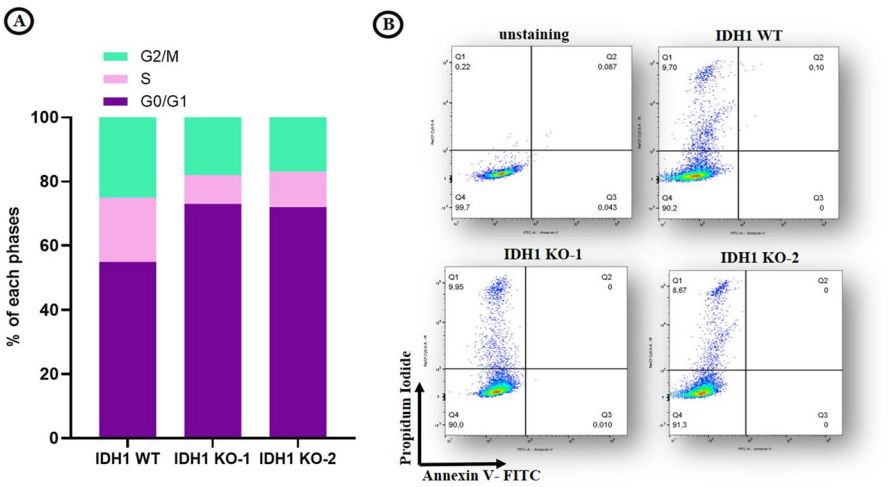

Fig. 5 The cells were arrested in the G0/G1 phase after IDH1 knockout. **A** The number of each cell cycle phase after PI staining was analyzed in the IDH1 WT and IDH1 KO1-2 cells. **B** The necrosis and apoptosis numbers of unstained, IDH1 WT and IDH1 KO1-2 cells. Q1: cells were stained with PI and Annexin V-FITC, and Q2: cells were stained with Annexin V-FITC

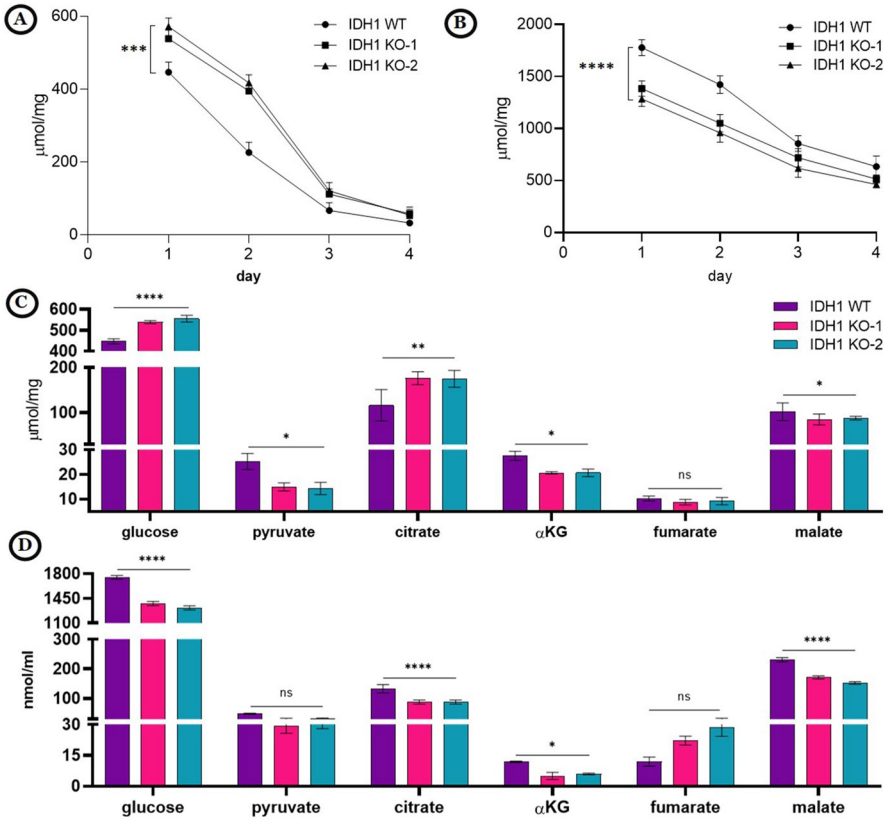

Fig. 6 Intracellular and extracellular metabolite levels in energy metabolism after IDH1 knockout. **A** Time-dependent intracellular and **B** extracellular glucose levels were calculated using the DNS method. The spectrophotometric method **was** used to calculate **C** Intracellular and **D** extracellular pyruvate levels. The HPLC method was used to determine **C** intracellular and **D** extracellular citrate, αKG, fumarate, and malate levels. *$p < 0.05$, **$p < 0.01$, ****$p < 0.0001$, ns: non-significant

The Effect of IDH1 Knockout on the Colon Cancer Metabolism

The intracellular and extracellular levels of metabolites in 1 million cells were profiled to investigate the metabolic changes in the IDH1 KO clones. The first part of energy production begins with converting glucose to pyruvate. The intracellular glucose level was 544,0 and 5662 µmol/mg in the IDH1 KO-1 and IDH1 KO-2, while it was determined as 4385 µmol/mg at 24 h, respectively (Fig. 6A). In addition, the time-dependent intracellular glucose was determined at 24–96 h (Fig. 6A). During the time, intracellular glucose level was higher in IDH1 KO clones than in IDH1 WT. The pyruvate synthesized as the end product in the glycolysis pathway is converted to Acetyl CoA and participates in the TCA cycle. Intracellular pyruvate level was 1.7 and 1.8 times reduced ($p < 0.05$) according to control, respectively (Fig. 6C). In the TCA cycle, the intracellular citrate level was 2.0- and 1.8-fold

increased ($p < 0.05$) in IDH1 KO1 and IDH1 KO2 compared to IDH1 WT, respectively. The intracellular αKG and malate levels were 1.4 and 1.5 times reduced in IDH1 KO1 and 1.5 and 1.3 times reduced ($p < 0.05$) in IDH1 KO2 compared to control, respectively. According to the control, the intracellular fumarate levels were not significantly changed in IDH1 KO clones (Fig. 6C).

The extracellular glucose was consumed more in the IDH1 WT than in IDH1 KO cells. The extracellular citrate, αKG, and malate levels were 1.3, 1.7, 2,4, and 1.3 times less released in the IDH1 KO-1 and 1.4, 1.6, 2.0, and 1.5 times less released ($p < 0.05$) in the IDH1 KO-2 according to control, respectively (Fig. 6D). According to the control, the extracellular pyruvate and fumarate levels were not significantly changed in IDH1 KO clones (Fig. 6D). In the time-dependent extracellular glucose level, it was less consumed in IDH1 KO clones than in IDH1 WT during 4 days (Fig. 6B).

Discussion

The IDH enzyme has a wide variety of functions, such as regulating the level of αKG and NADH, and thus plays an essential role in the cellular redox state (Cardaci and Ciriolo 2012). Until now, the role of the IDH enzyme in various types of cancer, including colorectal cancer, has been studied (Qiao et al. 2021; Li et al. 2019; Wang et al. 2020). Qiao et al. (2021) found that wt-IDH2 protects nuclear DNA from oxidative damage in colorectal cancer. Additionally, biochemical background in the concentration of 2-HG was investigated in breast cancer cells and they found that wt-IDH2 actively role in the 2-HG production pathway (Špačková et al. 2021). Another study confirmed that liver metastasis of colorectal cancer was inhibited by wt-IDH1 deacetylation (Wang et al. 2020). Our study aimed to investigate the role of the wt-IDH1 enzyme in the progression of colon cancer. The aggressive features of colon cancer cells were notably decreased when the IDH1 enzyme was depleted. The results showed that wt-IDH1 could be a potential therapeutic target in colon cancer.

Perturbating target genes offers various benefits, including improving approaches to novel targeted therapies, examining the role of mutations in metabolism, and performing detailed molecular and functional characterizations (Wu et al. 2020). Until now, different cell models have been developed with the CRISPR-Cas9 method in glioma (Moure et al. 2019), AML (Brabetz et al. 2017), and chondrosarcoma (Li et al. 2019) to investigate the roles of IDH1 enzymes in the different types of cancer pathogenesis. Li et al. (2019) perturbated mutant IDH1 and found that integrins were downregulated chondrosarcoma growth was impaired. The IDH1 gene was successfully depleted in our work, and a cell model was generated to evaluate the function of this gene in colon adenocarcinoma cell lines. The significant hallmarks of colon cancer were investigated in the IDH1 KO cells. The proliferation (Fig. 3B), invasion (Fig. 3C) and migration (Fig. 4A–B) abilities, and colony-forming capacity (Fig. 4C; Fig. 7) of these cells were significantly decreased in IDH1 KO clones compared to the control. In addition, the cell morphologies of IDH1 knockout cells were

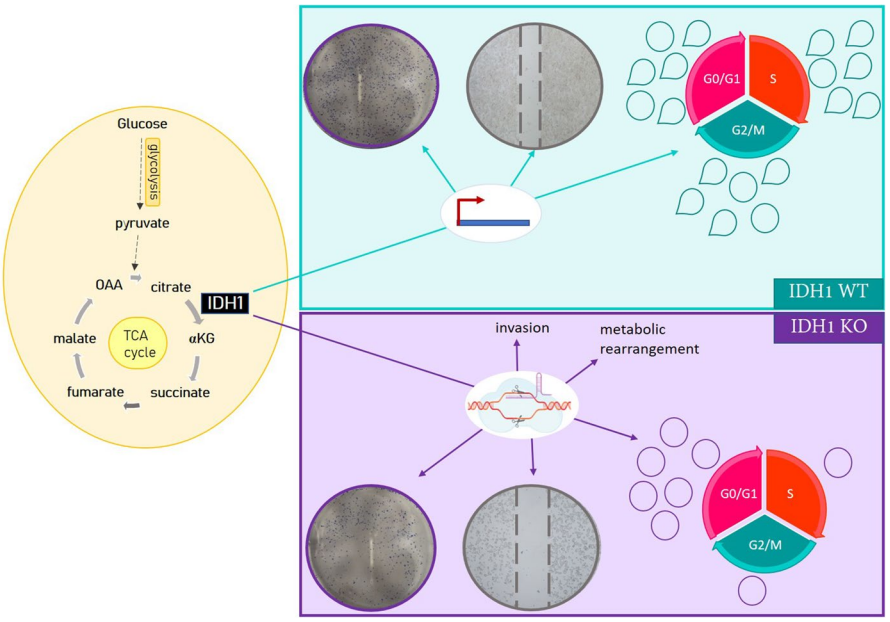

Fig. 7 The significant effect of IDH1 knockout on some hallmarks of colon adenocarcinoma cells. IDH enzymes perform decarboxylation of isocitrate to αKG, which further oxidizes to the succinate (Barnes et al. 1971). The upper and lower panels show the characteristics of cells containing wild-type and silenced IDH enzymes, respectively. CRISPR/Cas9 tool was utilized to knockout the IDH1 gene and IDH1 KO resulted in G0/G1 arrest, and reduced proliferation. In addition, the invasion, migration, and colony formation abilities of IDH1 KO clones were significantly decreased accompanied by morphological changes

significantly changed (Fig. 3A), and they were retained in G0/G1 phases (Fig. 5A; Fig. 7). It was hypothesized that since the decrease in the proliferation rate and the arrest in the G1 phase causes a decrease in energy production, the metabolic rearrangement in Glycolysis and TCA cycle was observed in the IDH1 KO clones. In the literature, features of mutant and wide-type IDH1 in the progression of cholangiocarcinoma have been studied. They found that cell proliferation, migration, and invasion capacities were decreased in IDH1 knockout cells (Su et al. 2020). In addition, our results are supported by the previous study. The IDH1 knockdown led to G1-phase arrest, reduced cell proliferation, and decreased invasion ability of colon cancer (Yang et al. 2021).

Cancer cells exhibit significant changes in many energy metabolisms (Hanahan and Weinberg 2011). Metabolic reprogramming occurs in basic mechanisms that support and/or direct cancer initiation, progression, and treatment response (Hanahan and Weinberg 2011). The development of an effective systemic therapy related to the metabolic rearrangement of colon cancer may give a new perspective to cancer treatments (Neitzel et al. 2020). In this study, both the intracellular and extracellular levels of metabolites in the TCA cycle and glycolysis were investigated in the IDH1 KO clones, and significant changes were observed. We

found that the knockout of the IDH1 induces an increase in intracellular glucose levels (Fig. 6A) due to less glucose participating in the TCA cycle. In this case, the decrease in the intracellular pyruvate level (Fig. 6C) in the IDH1 KO clones may be related to converting pyruvate to oxaloacetate to participate in the TCA cycle in mitochondria. Increased intracellular citrate and decreased αKG and malate levels (Fig. 6C) in IDH1 KO cells compared to control were directly associated with silencing the IDH1 gene. In the literature, a similar result about decreased αKG level was found in the IDH1 knockout cholangiocarcinoma cell lines. They also found that NADPH/$NADP^+$ ratio was also decreased after IDH1 silencing (Su et al. 2020).

Although the effects of the IDH1 gene on colon cancer were studied in only one cell line, significant results were obtained in two different clones. In the future, the effects of the IDH1 gene on colon cancer are planned to be studied on xenograft models of colon cancer.

In conclusion, the wtIDH1 gene was successfully silenced by CRISPR/Cas9 method and we continued with two IDH1 KO clones. Then the effect of IDH1 knockout on colon cancer progression was analyzed using different techniques. The results showed that IDH1 knockout affected the significant hallmarks of colon cancer. IDH1 knockout results in G0/G1 arrest, reduce proliferation, and decrease invasion, migration, and colony formation abilities. In addition, morphological changes and metabolic rearrangement were observed in IDH1 KO cells (Fig. 7). Our study showed that wt-IDH1 could be a potential therapeutic target in colon cancer.

Acknowledgements We gratefully thank doctoral student Ece Çakıroğlu for her contribution to the CRISPR/Cas9 method.

Author Contributions EBA performed the experiments and analyzed the data and writing- the original draft; SS analyzed the data in the CRISPR/Cas9 method and Writing—review & editing; HAK coordinated all aspects of this work, Writing—review & editing, Supervision HAK contributed to the study conception and design.

Funding The authors declare that there were not any funds, grants, or other support during the preparation of this manuscript.

Data Availability All the generated or analyzed datas during the current study are included in this manuscript. The datas in the present study are available from the corresponding author on reasonable request.

Declarations

Conflict of ınterest There have no relevant financial or non-financial interests by all the authors.

References

Alavi M, Rai M (2021) Antisense RNA, the modified CRISPR-Cas9, and metal/metal oxide nanoparticles to inactivate pathogenic bacteria. CMBR 1:52–59

Atalay EB, Kayali HA (2022) The elevated D-2-hydroxyglutarate level found as a characteristic metabolic change of colon cancer in both in vitro and in vivo models. Biochem Biophys Res Commun 627:191–199. https://doi.org/10.1016/j.bbrc.2022.08.019

Ayar Kayali H, Tarhan L (2006) Vancomycin antibiotic production and TCA-glyoxalate pathways depending on the glucose concentration in Amycolatopsis orientalis. Enzyme Microb Technol 38:727–734
Barnes LD, Kuehn GD, Atkinson DE (1971) Yeast diphosphopyridine nucleotide specific isocitrate dehydrogenase purification and some properties. Biochem 10:3939–3944
Biedermann J, Preussler M, Conde M, Peitzsch M, Richter S, Wiedemuth R (2019) Mutant IDH1 differently affects redox state and metabolism in glial cells of normal and tumor origin. Cancers 11:2028
Bin H, Mei H, Hui W, Bing Z (2022) The correlation between miR -34a-3p, miR -31, PLEK2 and the occurrence, development and prognosis of colorectal cancer. Cell Mol Biol (noisy-Le-Grand) 68:192–200
Brabetz O, Alla V, Angenendt L, Schliemann C, Berdel WE, Arteaga MF, Mikesch JH (2017) RNA-guided CRISPR-Cas9 system-mediated engineering of acute myeloid leukemia mutations. Mol Ther Nucleic Acids 6:243–248
Cardaci S, Ciriolo MR (2012) TCA cycle defects and cancer: when metabolism tunes redox state. Int J Cell Biol. https://doi.org/10.1155/2012/161837
Crooks DR, Maio N, Lang M, Ricketts CJ, Vocke CD, Gurram S, Turan S, Kim YY, Cawthon GM, Sohelian F, Val N, Pfeiffer RM, Jailwala P, Tandon M, Tran B, Fan TMW, Lane AN, Ried T, Wangsa D, Malayeri AA, Merino MJ, Yang Y, Meier JL, Ball MW, Rouault TA, Srinivasan R, Linehan WM (2021) Mitochondrial DNA alterations underlie an irreversible shift to aerobic glycolysis in fumarate hydratase–deficient renal cancer. Sci Signal 14:eabc4436
Dalziel K (1980) Isocitrate dehydrogenase and related oxidative decarboxylases. FEBS Lett 117:45–55
Dang L, White DW, Gross S, Bennett BD, Bittinger MA, Driggers EM, Fantin VR, Jang HG, Jin S, Keenan MC, Marks KM, Prins RM, Ward PS, Yen KE, Liau LM, Rabinowitz JD, Cantley LC, Thompson CB, Vander Heiden MG, Su SM (2009) Cancer-associated IDH1 mutations produce 2-hydroxyglutarate. Nature 462:739–744
Franken NA, Rodermond HM, Stap J, Haveman J, Van Bree C (2006) Clonogenic assay of cells in vitro. Nat Protoc 1:2315–2319
Hanahan D (2022) Hallmarks of cancer: new dimensions. Cancer Discov 12:31–46
Hanahan D, Weinberg RA (2011) Hallmarks of cancer: the next generation. Cell 144:646–674
Hao HX, Khalimonchuk O, Schraders M, Dephoure N, Bayley JP, Kunst H, Devilee P, Cremers CWRJ, Schiffman JD, Bentz BG, Gygi SP, Winge DR, Kremer H, Rutter J (2009) SDH5, a gene required for flavination of succinate dehydrogenase, is mutated in paraganglioma. Sci 325:1139–1142
Hao J, Wei H, Qi Y, Liu H (2022) miR-129-5p plays an anticancer role in colon cancer by targeting RSF1. Cell Mol Biol 67:196–201
Jinek M, Chylinski K, Fonfara I, Hauer M, Doudna JA, Charpentier A (2012) A programmable dual-RNA-guided DNA endonuclease in adaptive bacterial immunity. Sci 337:816–821
Khuwijitjaru P, Koomyart I, Kobayashi T, Adachi S (2017) Hydrolysis of konjac flour under subcritical water conditions. Chiang Mai J Sci 44:988–992
Krebs H, Johnson WA (1937) The role of citric acid in intermediate metabolism in animal tissues. Enzymologia 4:148–156
Li L, Xiaoyu H, Trent JC (2019) Depletion of mutant IDH1 impairs chondrosarcoma growth by down-regulating integrins. J Clin Oncol 37:11031–11031
Livak KJ, Schmittgen TD (2001) Analysis of relative gene expression data using real-time quantitative PCR and the $2-\Delta\Delta CT$ method. Methods 25:402–408
Moure CJ, Diplas BH, Chen LH, Yang R, Pirozzi CJ, Wang Z, Spasojevic I, Waitkus MS, He Y, Yan H (2019) CRISPR editing of mutant IDH1 R132H induces a CpG methylation-low state in patient-derived glioma models of G-CIMP. Mol Cancer Res 17:2042–2050
Neitzel C, Demuth P, Wittmann S, Fahrer J (2020) Targeting altered energy metabolism in colorectal cancer: oncogenic reprogramming, the central role of the TCA cycle and therapeutic opportunities. Cancers 12:1731
Pollard PJ, Ratcliffe PJ (2009) Puzzling Patterns of Predisposition. Sci 324:192–194
Qiao S, Lu W, Glorieux C, Li J, Zeng P, Meng N (2021) Wild-type IDH2 protects nuclear DNA from oxidative damage and is a potential therapeutic target in colorectal cancer. Oncogene 40:5880–5892
Ran FA, Hsu PD, Wright J, Agarwala V, Scott DA, Zhang F (2013) Genome engineering using the CRISPR-Cas9 system. Nat Protoc 8:2281–2308
Shi J, Fan L, Li B, Pan H (2022) Molecular Mechanism of Integrin αvβ6 in Liver Metastasis of Colon Cancer Based on SDF-1/CXCR4. Cell Mol Biol 67:88–95
Sjöblom T, Jones S, Wood LD, Parsons DW, Lin J, Barber TD (2006) The consensus coding sequences of human breast and colorectal cancers. Sci 314:268–274

Špačková J, Gotvaldová K, Dvořák A, Urbančoková A, Pospíšilová K, Větvička D, Leguina-Ruzzi A, Tesařová P, Vítek L, Ježek P, Smolková K (2021) Biochemical background in mitochondria affects 2HG production by IDH2 and ADHFE1 in breast carcinoma. Cancers 13:1709

Su L, Zhang X, Zheng L, Wang M, Zhu Z, Li P (2020) Mutation of isocitrate dehydrogenase 1 in cholangiocarcinoma impairs tumor progression by inhibiting isocitrate metabolism. Front Endocrinol 11:189

Subasi E, Atalay EB, Erdogan D, Sen B, Pakyapan B, Ayar Kayalı H (2020) Synthesis and characterization of thiosemicarbazone-functionalized organoruthenium (II)-arene complexes: Investigation of antitumor characteristics in colorectal cancer cell lines. Mater Sci Eng C 106:110152

Sung H, Ferlay J, Siegel RL, Laversanne M, Soerjomataram I, Jemal A, Bray F (2021) Global cancer statistics 2020: GLOBOCAN estimates of incidence and mortality worldwide for 36 cancers in 185 countries. CA Cancer J Clin 71:209–249

Wang B, Ye Y, Yang X, Liu B, Wang Z, Chen S (2020) SIRT 2-dependent IDH 1 deacetylation inhibits colorectal cancer and liver metastases. EMBO Rep 21:e48183

Wen L, Zhang Y, Yang B, Han F, Ebadi AG, Toughani M (2020) Knockdown of Angiopoietin-like protein 4 suppresses the development of colorectal cancer. Cell Mol Biol 66:117–124

Wu SS, Li QC, Yin CQ, Xue W, Song CQ (2020) Advances in CRISPR/Cas-based gene therapy in human genetic diseases. Theranostics 10:4374

Xi Y, Xu P (2021) Global colorectal cancer burden in 2020 and projections to 2040. Transl Oncol 14:101174

Yang H, Xie S, Liang B, Tang Q, Liu H, Wang D, Huang G (2021) Exosomal IDH1 increases the resistance of colorectal cancer cells to 5-Fluorouracil. J Cancer 12:4862

Yoo KS, Lee EJ, Patil BS (2011) Underestimation of pyruvic acid concentrations by fructose and cysteine in 2, 4-dinitrophenylhydrazine-mediated onion pungency test. J Food Sci 76:C1136–C1142

Authors and Affiliations

Esra Bulut Atalay[1,2] · Serif Senturk[1,2] · Hulya Ayar Kayali[1,2,3]

[1] Izmir Biomedicine and Genome Center, Izmir 35340, Turkey

[2] Izmir International Biomedicine and Genome Institute (IBG), Dokuz Eylül University, Mithatpasa St. No: 58/5, Balcova, 35340 Izmir, Turkey

[3] Department of Chemistry, Division of Biochemistry, Faculty of Science, Dokuz Eylul University, 35160 İzmir, Turkey